Journal of Physics:
Conference Series

PAPER • **OPEN ACCESS**

Assessment of synthetic turbulence of stably stratified atmospheric boundary layers for LES

To cite this article: Hugo Olivares-Espinosa and Johan Arnqvist 2024 *J. Phys.: Conf. Ser.* **2767** 092109

Journal of Physics: Conference Series **2767** (2024) 092109 doi:10.1088/1742-6596/2767/9/092109

Assessment of synthetic turbulence of stably stratified atmospheric boundary layers for LES

Hugo Olivares-Espinosa and Johan Arnqvist

Uppsala University, Department of Earth Sciences, Wind Energy Section, Cramérgatan 3, 621 67 Visby, Sweden

E-mail: hugo.olivares@geo.uu.se

Abstract.

This work studies the evolution of turbulence in a Stable Boundary Layer (SBL) in Large-Eddy Simulations (LES) when a synthetic turbulence field of velocity and temperature is used as initial condition and as well as precursor. Following common approaches found in the literature, initial fields of different characteristics are created and their evolution in the LES is evaluated in order to assess the ability of the synthetically generated turbulence to represent a snapshot of SBL turbulence. The study is carried out with two modelling cases, a forested site as well as the GABLS benchmark [4]. In both cases, the usage of a turbulent SBL as an initial condition proved advantageous to reach a faster convergence presenting an opportunity for computational savings. Yet, the very different turbulence conditions of the modelling setups produce varying results with regard to the type of velocity and temperature fluctuations. Likewise, the usage of a precursor was shown able to represent the flow in a successor LES although with varying reliability, dependent on the background turbulence and the stratification level, that suppresses velocity fluctuations and could lead to the misrepresentation of turbulence level.

1. Introduction

Accuracy in the simulation of atmospheric flows in the wind industry is to a large extent limited by computational times. The need for "overnight" solutions has largely inhibited the usage of the high-fidelity models such as those required to represent the dynamics of the Atmospheric Boundary Layer (ABL) and its interaction with wind turbines in parks. As the restrictions are increased by the need for repeating the process for multiple configurations, calculation standards have been developed for the representation of the wind flow. Among the available methods of generation, the one by Mann [1] is widely used in both research and industrial applications for its capability of generating physically coherent velocity fields, although restricted to represent stratified flows by modifying the model parameters and lacking the ability to produce temperature fluctuations. The latter becomes problematic when the synthetic turbulence is directly used for the assessment of turbine/park performance under various stability conditions. In the case of Large-Eddy Simulations (LES), complications arise when the synthetic

field is employed as a starting field or to derive boundary conditions in non-neutral stratification, since that requires physically consistent relations between fluctuations in all three velocity components as well as the temperature. The challenge of extending the Mann model to comprise the generation of stratified turbulence, that includes a temperature field, has been taken upon by different authors, such as Segalini and Arnqvist [2] or Chougule et al. [3]. In this work, we assess commonly used strategies that employ a synthetically generated turbulence flow to simulate an ABL flow with LES for the specific case of stable stratification. These comprise the usage of the synthetic turbulence either as an initial field or in the so called "box" configuration –normally employed instead of a precursor–. We follow the evolution of the turbulence field in its path to reach statistical convergence and evaluate how long the different strategies take to achieve such state, while also assessing their accuracy to represent the stable ABL.

2. Modelling cases

Two different modelling scenarios have been chosen to assess the development of the flow under the different initial conditions. The first one is a forested case, where the wind flow over a cooling homogeneous canopy is modelled with LES. The second one is the widely-used GABLS benchmark dedicated to evaluate the performance of LES models to represent a Stable Boundary Layer (SBL) driven by a uniform geostrophic wind over a flat ice surface [4].

Forests are an area of interest for the development of wind parks, while representing challenging conditions for their performance. To represent the enhanced level of turbulence arising from the trees, a simple approach would consist of using a large aerodynamic roughness z_0, which in turn demands a minimum height of the first cell node z_1 above the ground, away from the roughness sublayer where Monin-Obukhov is not applicable. This issue is discussed by [5] where it is argued that in order to assure that z_1 is within the inertial sublayer then $z_1 > 50z_0$. The fulfillment of this requirement might be undesirable, for example, to avoid the abrupt change in cell heights above the wall or because the value of z_0 varies over the ground, such as when heterogeneous vegetation is present over the terrain. This issue can be avoided by conceiving the forest as a porous surface and modelling its drag. With the purpose of studying the usage of synthetic turbulence fields in LES on these regions, the conditions of the Ryningsnäs site in south-east Sweden are reproduced. This is a forested location at a latitude of 57°N with a mean canopy height of $h_f = 20$ m, where tower measurements are available from heights between 40 m and 138 m above ground. A description of the site and the measurement campaign can be found on [6]. Complementary data is also obtained from the similar forested site of Hornamossen, also in Sweden [7]. The experimental data is selected based on the criteria for stable near neutral described in [6].

GABLS is based on the simulations of a SBL on arctic conditions [8], the case definition and the results of the LES intercomparison are found on [4]. The main details of the setup are: a computational domain of $400 \times 400 \times 400$ m^3 with initial potential

temperature of 265 K up to 100 m and random fluctuations of amplitude 0.1 K applied below 50 m, followed by a capping inversion of 0.01 K/m. The bottom surface is a no-slip wall with a roughness of $z_0 = 0.1$ m that cools at a constant rate of 0.25 K/h. The flow is driven as to maintain a westward (along the $x-$axis) geostrophic wind $U_g = 8$ m/s with the initial velocity field set equal to this. A Coriolis force is also included, corresponding to a latitude of 73°N. The LES is run for 9 h of simulated time, using the results of the final hour for the comparison.

3. Model description

3.1. Synthetic turbulence

When creating a turbulent and stratified ABL as starting conditions for LES, two different strategies are initially examined. The first approach consists in perturbing only the modelled temperature field [9] thus allowing the LES model itself to develop turbulence in the wind field. The second strategy is to provide synthetic turbulence by a Rapid Distortion Theory simulator that includes stratification effects [2, 7] . The synthetic turbulence fields may then be manipulated to match the mean properties of the initial fields, such as variance and covariance magnitudes or the presence of an Ekman spiral.

As an initial step, boxes of synthetic turbulence were created by the solution of the Rapid Distortion Theory (RDT) equations [2]. The solution generates the 3-dimensional spectral tensor for u, v, w and θ. The actual synthetic fields are later created by the inverse fast Fourier transform of the tensor, as in [1]. The input data required for the model are: wind shear, α, Brunt-Väisälä frequency, N, velocity turbulence scale, u_s, temperature turbulence scale, θ_s, turbulence length scale, L_s, number of grid points in each direction, $[N_x,\ N_y,\ N_z]$ and box size, $[L_x,\ L_y,\ L_z]$. In the final step, synthetic fluctuations are rescaled and mean background profiles are added to the fluctuations. The background profiles are created by setting the boundary layer height according to [10] which was used together with Ekman layer profiles from [11] whereas for temperature, an integration of the eddy viscosity using a turbulent Prantl number of 0.83 and a linear vertical decay of the heat flux according to [12]. To facilitate a comparison with observational data, the values of the input data are obtained from the Ryningsnäs observations described by [6].

3.2. LES model

LES are run on OpenFOAM v3.0.1 [13] on an incompressible solver employing the Boussinesq approximation to represent the effects of buoyancy. The Sub-Grid Scale model (SGS) of Deardorff [14] as revised by Moeng [15] is used, which accounts for the stratification effects in the calculation of the turbulence viscosity $\nu_t = 0.1\sqrt{k_{\mathrm{SGS}}}l$ via a mixing lengthscale l. A wall model based on the Schumann surface stress [16] in combination with a heat-flux model that estimates the wall heat-flux in function

of the wall temperature and its difference with the air above. The latter follows the approach recommended by [17] to avoid prescribing a wall-heat flux that can otherwise overestimate the friction velocity in stable stratification. The SGS and wall model implementations discussed above are available in the SOWFA libraries for OpenFOAM [18], we make use of these with some modifications, in particular for the forest modelling. The drag effect of the forest on the wind flow is modelled employing source terms in the momentum and SGS equations whereas the cooling of the air above the forest is achieved via a source term in the temperature equation [19]. Details of the model and its implementation can be found in [20].

3.3. Numerical setup

Five turbulence fields of velocity and temperature are created for each setup, four are used as initial conditions of calculations using periodic conditions (identified with labels IC) while another (TB) is used as a turbulence box of a successor LES. The numerical setup for the forest cases is presented first, followed by that for GABLS.

	FIC1	FIC2	FIC3	FIC4	FTB
U_0	Ekman	Ekman	Uniform U_g	Uniform U_g	Ekman
θ_0	Stable	Stable	Stable	Neutral	Stable
u', v', w'	2D rot., N1984	None	None	None	2D rot., N1984
θ'	N1984	N1984+ME2015	N1984+ME2015	Random	N1984

Table 1: Sets of initial conditions of velocity and potential temperature for the forest cases. 2D rotated indicates rotation to the local mean wind direction, N1984 indicates scaling of the variance with height according to Nieuwstadt 1984 [12] and N1984 + ME2015 indicates that the temperature fluctuations were additionally scaled with U_g^2 divided by the Eckert number 0.16.

In the forest simulations, the synthetic fields FIC1 to FIC4 are used as initial conditions and thus have the same dimensions as the LES: $L_x \times L_y \times L_z = 3584$ m $\times$ 896 m $\times$ 1024 m. The resolution used by the turbulence generator is uniform in the horizontal direction $\Delta_x, \Delta_y = 7$ m while also constant vertically with $\Delta_z = 2$ m. The synthetic fields are generated as described in Sec. 3.1 with the main parameters listed in Table 1, with values $z_0 = 3.0$ m, a longitudinal ($\varphi = 270$) $U_g = 12.4$ m/s and a displacement height of $d = 13$ m (the value at which the logarithmic profile is zero with respect to z_0, located below the canopy top). The boundary layer height is $H = 277$ m with a capping inversion of 0.01 K/m set above it. The cell resolution in the LES is equal to the synthetic fields in the horizontal direction, vertically it is also the same up to $z = 320$ m, stretching uniformly from there so the last cell is about 39 m in height. The initial fields for each calculation are created by linear interpolation between the synthetic fields and the LES meshes. Cases FIC1 to FIC3 attempt to model a stratified SBL from the onset while FIC4 is initiated with a neutrally stratified and uniform

velocity. In the latter case, $\theta = 264.5$ K corresponding to the mean of the stratified $\theta(z)$ profile (FIC1 to FIC3) between 20 m and 200 m. In the FTB case the synthetic field serves as a turbulence box of a subsequent successor simulation, this box has a domain of equal crosswise dimensions and cell resolution as previous FIC fields but with $L_x = 28672$ m. Following the Taylor hypothesis and assuming that the flow moves at the geostrophic velocity, FTB would represent a wind flow lasting $L_x/U_g = 2312.3$ s. Using the same initial conditions of FIC1, a period of 1 h is simulated so the remainder interval is recycled from the beginning of the box.

The LES comprise a forest of constant height h_f over a flat ground of $z_0 = 0.01$ m with a flow driven by a constant pressure gradient in the longitudinal direction with at U_g including a Coriolis force for the latitude of Rynigsnäs. The cooling of the SBL is produced by applying a net radiation Q_h at the canopy top of -52.7 W/m^2 (derived from measurements at 40 m [6]), equal to -0.419 K/m^2, with an ground temperature of T_g of 263 K. In cases FIC3 and FIC4 that use an initial neutral temperature profile, T_g extends up to the capping inversion. In all forest cases, the T_g remains constant during the simulations.

	GIC1	GIC2	GIC3	GIC4	GTB
U_0	IC4@8h	IC4@8h	Uniform U_g	Uniform U_g	IC4@8h
θ_0	IC4@8h	IC4@8h	Neutral	Neutral	IC4@8h
u', v', w'	2D rot., N1984	None	None	None	2D rot., N1984
θ'	N1984	N1984+ME2015	N1984+ME2015	Random	N1984
t_0	8 h	8 h	0 h	0 h	8 h

Table 2: Sets of initial conditions of velocity and potential temperature for GABLS cases.

The GABLS cases are designed around the parameters of turbulence generation similar to the forest tests, so they are identified by analogous labels. The case definition employed in the benchmark [4] outlined in Sec. 2 is followed. Different cubic cell resolutions are employed there, ranging from 1 m to 12.5 m. The intermediate value of 3.125 m is used here as representative of LES used in wind energy calculations. Five synthetic turbulence fields are created following the methodology of Sec. 3.1 with the main parameters are listed in Table 2. Four cases, GIC1 to GIC4, assess the evolution of the flow according to different initial conditions. Hence, the size and resolution of the synthetic fields is as in the LES domain. GIC4 corresponds to the canonical GABLS case as prescribed in [4] while case GIC3 differs in that initial synthetic turbulence conditions are added that should permit the flow to attain a faster statistical convergence.

Cases GIC1, GIC2 and GTB attempt to model the turbulence conditions of the SBL at 8h so they can be compared with GIC3 and GIC4 during the succeeding 1 h period. Instead of modelling the mean profiles of velocity and temperature in the SBL as in the forest case, they are extracted from the results of GIC1 at the hour 8 (horizontal

means of 30-min averages) and subsequently adding the fluctuations. GIC1, GIC2 and GTB start with $T_g = 263$ K, the value after 8 h of cooling. Using the mean flow solution for these cases has the advantage of testing the adequacy of the synthetic fluctuations to represent the turbulence flow, as it is not affected by the adjustment of an otherwise flow parametrization to the conditions enforced by the pressure gradient and Coriolis force. The case GTB is analogous to FTB, where the synthetic field is used as a turbulence box for the successor LES, so crosswise dimensions and cell resolution are equal to the GIC fields but $L_x = 25600$ m. GTB covers a span of $L_x/U_g = 3200$ s but since 1 h is simulated, the remaining 400 s are taken from the beginning of the box. The initial conditions in the LES of GTB are equal to those of GIC1. The starting time of each calculation with respect to the duration of the regular GABLS of 9 h is also shown in Table 2.

Other than stated above, all LES are carried out on domains with the same boundary conditions except that in the IC cases all side boundaries are set to periodic while in the TB case only the lateral boundaries are periodic, the planes of turbulence (velocity and temperature) are introduced at the inlet while the outlet employs a Neumann boundary condition. All cases are run with a time-step of $\Delta t = 0.15$ s except the successor simulations that employ an adaptive time-step as to maintain CFL $\lesssim 0.8$ that gives $\overline{dt} \simeq 0.15$ s for GTB and $\overline{dt} \simeq 0.07$ s for FTB.

4. Results

The analysis begins by observing the evolution of the flow for each of the configurations shown in Table 1. For the forest LES, Fig. 1 shows the velocities, k_{res} and the wind directions for 7 vertical positions located along the central column of each domain. FIC1-FIC4 shows 6 h from the onset while FTB shows the 1 h duration of the synthetic precursor. The first noticeable difference is the development of the velocity profile by the cases starting with uniform velocity FIC3 and FIC4. However, this adjustment of the flow is also observed in cases FIC1 and FIC2 for about the same duration that is also observed in the wind direction, indicating that the starting U_0 profile is not an exact match for the forces driving the flow. Statistical convergence of the flow is qualitatively assessed with k_{res} whose results also show the increase and decrease in the FIC3 and FIC4 cases during the first hours of the simulation until they set to about the same levels as the rest of cases at about 5 h.

Interestingly, the successor simulation maintains the flow values at each level during the 1 h simulation while only showing a quick adjustment of the k_{res} during the first minutes. The cooling of the forest does increase the stratification of the SBL, as it can be seen in the temperature profiles in Fig. 2 but the turbulence arising from the forest drag seem to inhibit the changes in velocity and TKE. Indeed, the profiles of total TKE, $k_{tot} = k_{res} + k_{\mathrm{SGS}}$ only appreciably change for the cases using an initial uniform velocity FIC3 and FIC4. For those, the usage of a stable θ_0 and additional fluctuations θ' do not appear to have a strong impact in the flow development, supporting the argument

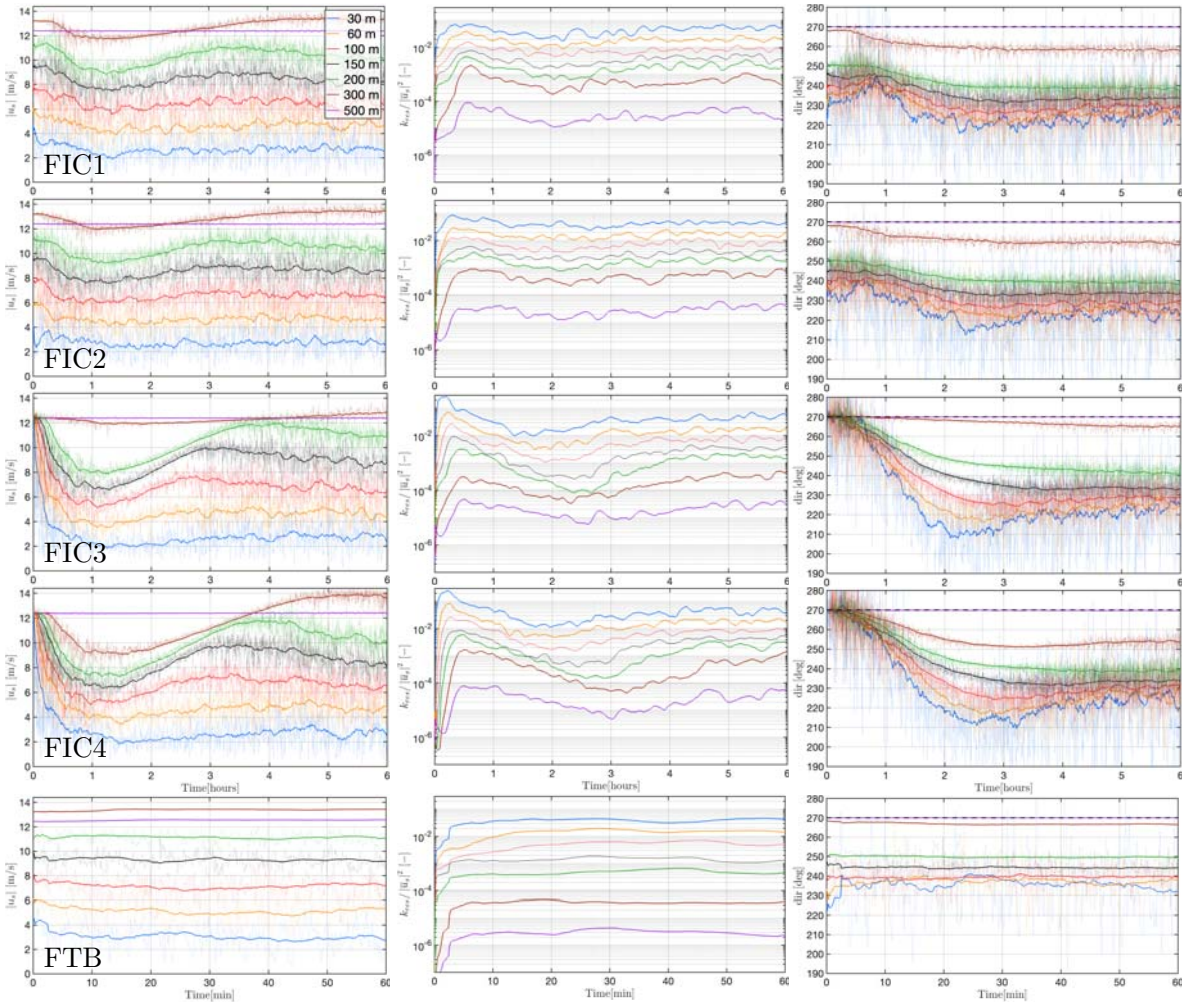

Figure 1: Evolution of the horizontal velocity magnitude, resolved TKE and wind direction at various vertical positions. Results for the different cases of Table 1 are presented in each row. Solid lines representing a 10-min window average are drawn over their corresponding time-series.

regarding the large turbulence over the canopy. Moreover, these cases show a drop in temperature near the ground to about 260 K which is not observed in the other simulations. This dip is maximum at about 3 h with θ increasing after this. Since the ground temperature is constant at 263 K, the cooling of the forest overcomes the speed at which the ground heat-flux can increase the temperature above it until the difference is large enough for the same heat flux to increase and raise θ. In the case of FTB, while it is apparent that flow properties are largely maintained during the simulation period, k_{tot} reveals that the absolute TKE is smaller than in longer simulations, an indication that the flow characteristics could still change if the sampling region was located at a larger distance from the inlet. Fig. 3 show the evolution of the one-point co-spectra at an elevation of 100 m for the LES and measurements from Ryningsnäs and Hornamossen. There is an a reduction in TKE in essentially all cases when moving

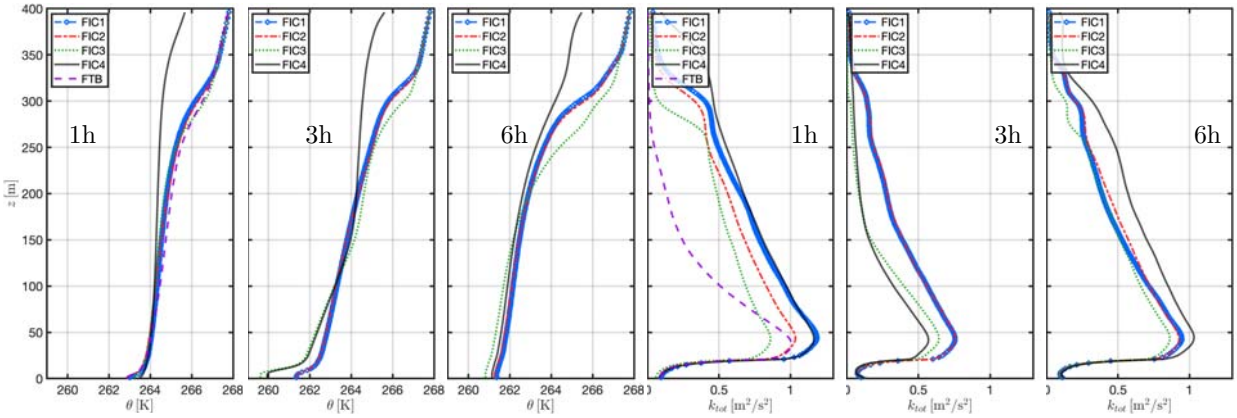

Figure 2: Profiles of potential temperature and total TKE obtained as the horizontal average over the domain for each cell height and time averaged during the preceding 30-min to the corresponding time.

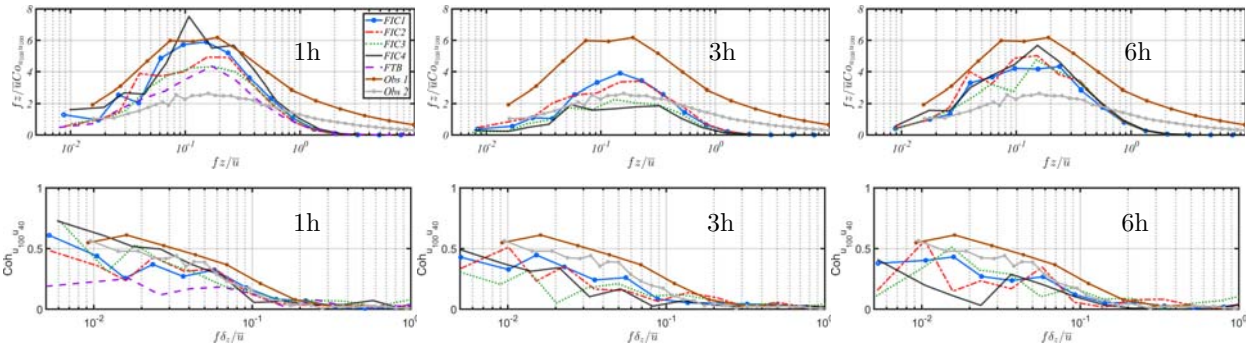

Figure 3: Top row: spectra of longitudinal velocity at 100 m. Bottom row: spectral coherence of longtudinal velocities at 40 m and 100 m. *Obs. 1* comes from measurements at Ryningsnäs while *Obs. 2* corresponds to Hornamossen. δ denotes vertical separation.

from 1 h to 3 h, before the values increase again at 6 h. The relative differences in TKE between the different cases are consistent with the observations made for k_{tot} in Fig. 2. While it is difficult to discern a change in the distribution of turbulence energy along the frequencies, it can be seen that the spectral energy follows the shape of the experimental results. Moreover, the amount of energy is between the measurements for the majority of cases. Fig. 3 also shows the evolution of the vertical coherence (calculated as in [21]) between the positions 40-100 m. The coherence stays relatively similar with respect to time, unlike the differences in turbulence level seen before between 1, 3 and 6 h. Notably, the coherence of FTB is markedly lower than the rest, indicating not only the transition from the synthetic turbulence to the LES but also that turbulence is still evolving at the sampling location. As in the previous case, the irregularity in the curves makes it difficult to distinguish variations with respect to the frequency.

Next, Fig. 4 shows the results for the different conditions to simulate GABLS presented in Table 2. The observations are restricted to the period of hours 8 to 9,

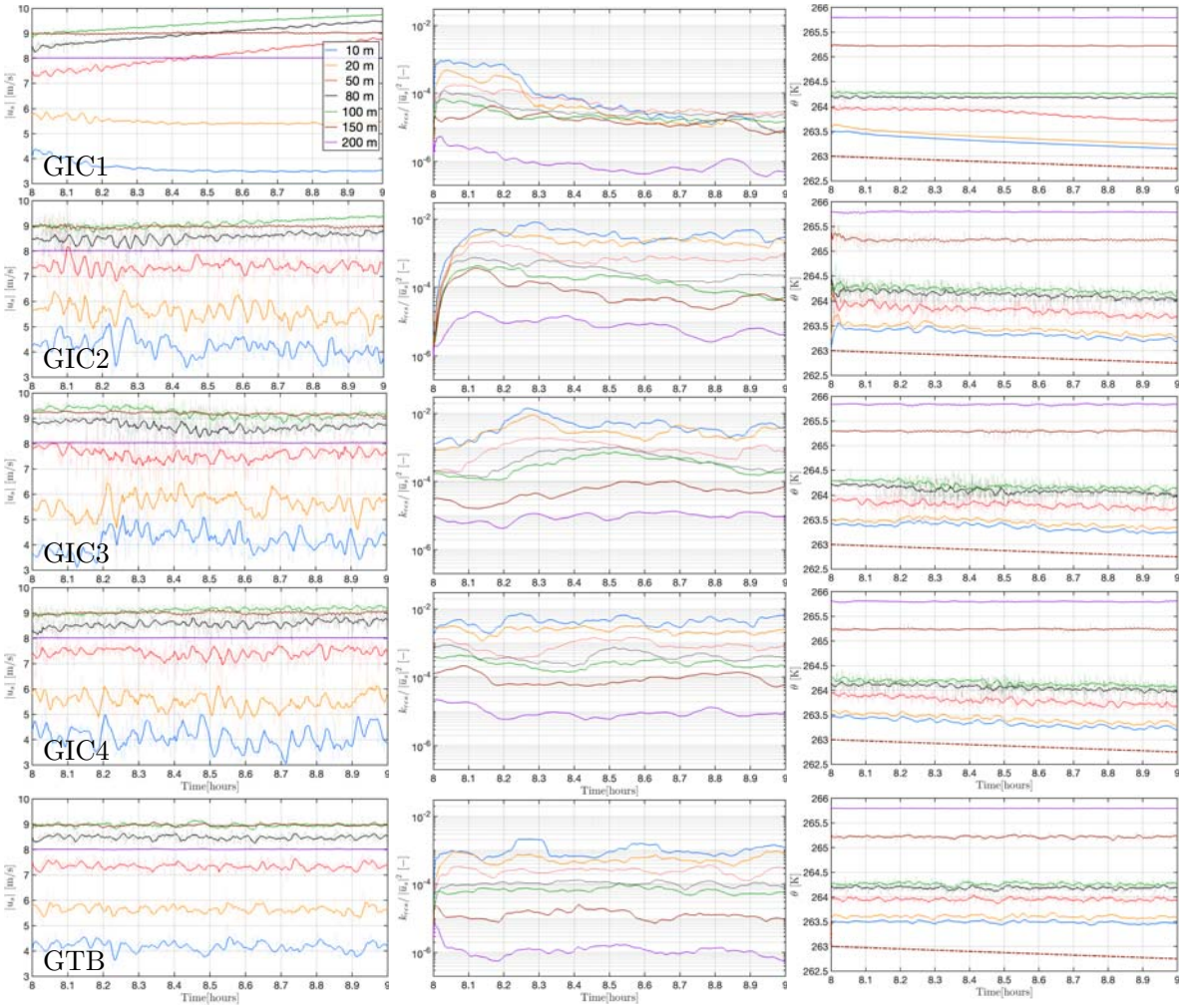

Figure 4: Evolution of the horizontal velocity magnitude, resolved TKE and potential temperature at various vertical positions. Results for the different cases of Table 2 are presented in each row. Solid lines representing a 10-min window average are drawn over their corresponding time-series.

so the period leading to that point simulated in cases GIC3 and GIC4 is not shown. Likewise, the study focuses on the differences in flow evolution so no comparison with the results from [4] is made. In the absence of the large turbulence from the forest of the previous case, the role of stratification is more important and some differences emerge (note that figures of θ are shown instead of wind direction). While GIC2 and GIC2 start with the same Ekman layer (extracted from GIC4 at 8h), the stronger fluctuations θ' in GIC2 permit to simulate a flow very closely to that predicted GIC4 itself. Meanwhile, the intial perturbations in GIC1 seem insufficient to be sustained in the SBL, leading to a noticeable reduction of TKE. The utilization of stronger temperature fluctuations in GI3 compared to GIC4 is rather unnoticed in the period from 8 h to 9 h but does lead to a quicker onset of turbulence at the start of the simulation. Fig. 5 shows the

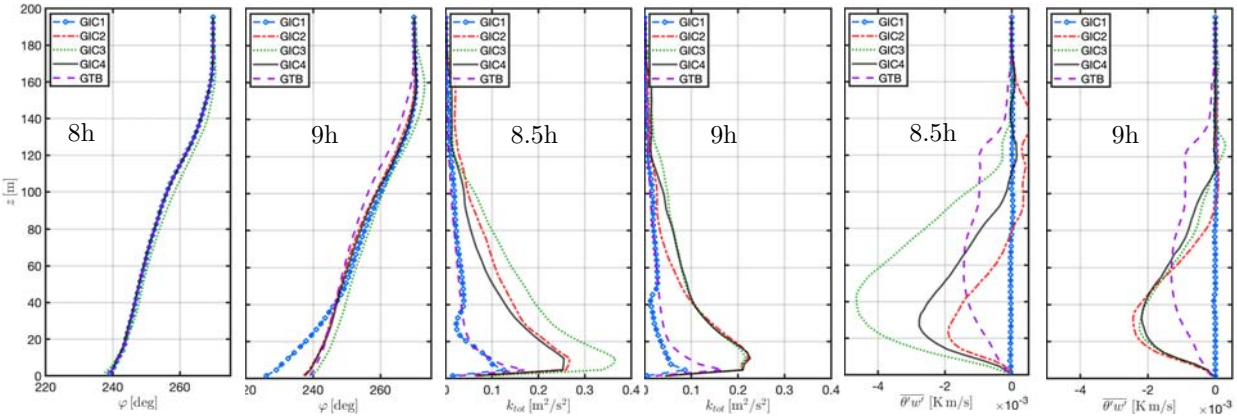

Figure 5: Profiles of wind direction, total TKE and vertical heat-flux obtained as the horizontal average over the domain for each cell height and time averaged during the preceding 30-min to the corresponding time.

differences in wind direction, k_{tot} and vertical heat flux. It is seen that the reduction of turbulence in GIC1 leads to a overprediction of the wind turning near the ground, the same reduction of TKE is observed in GTB but the wind direction is still matched at 9 h. GIC3 shows a higher TKE level and vertical flux at 8.5 h, but they become the same as GIC2 and GIC4 at 9 h while that of GTB is consistently lower and that of GIC1 essentially zero. The usage of a precursor seem to conduct to a less turbulent flow, noticeable both in the levels of k_{res} in Fig. 1 and k_{tot} in Fig. 5.

Conclusions

This work studied the evolution of turbulence in a Stable Boundary Layer (SBL) in a Large-Eddy Simulations (LES) under a number of strategies of field initialization and the usage of a precursor. The study was carried out to observe the differences in the simulation of an idealized forest and the widely known GABLS [4] benchmark. The forest simulation shows a faster convergence when a turbulent SBL is used for initialization, although the large turbulence generated from the forest drag reduces potential variations when different temperature fluctuations are used. Conversely, it was shown that such variations have an effect in the SBL flow of the GABLS case, permitting to represent an advanced stratification state in the flow that can be used as a starting point in the LES, leading to potentially large computational savings. The usage of the synthetic turbulence as a precursor was shown able to represent the flow in a successor LES although with varying reliability, dependent on the background turbulence and the stratification level, that suppresses velocity fluctuations and could lead to the misrepresentation of turbulence kinetic energy. Since this is a method of turbulence generation employed in the assessment of wind turbine and park performance, e.g. power and load calculations, special attention should be paid to avoid flaws in such estimations.

Acknowledgements: The computations of this work were performed in resources provided by the National Academic Infrastructure for Supercomputing in Sweden (NAISS).

References

[1] Mann J 1998 *Probabilistic Eng. Mech.* **13** 269-282.
[2] Segalini A and Arnqvist J 2015 *J. Fluid Mech.* **781** 330-352.
[3] Chougule A, Mann J, Kelly M and Larsen G C 2017 *Journal of the Atmospheric Sciences* **74** 4:949-74.
[4] Beare R J, Macvean M K, Holtslag A A M et al. 2006 *Boundary-Layer Meteorol* **118** 247–272
[5] Basu S and Lacser A 2017 *Boundary-Layer Meteorol* **163** 351–355
[6] Arnqvist J, Segalini A, Dellwik E, Bergström H 2015 *Bound.-Lay. Meteorol.* **156** 53-71.
[7] Mohr M, Arnqvist J, Abedi H, Alfredsson H, Baltscheffsky M, Bergström H, Carlén I, Davidsson L, Segalini A and Söderberg S 2018. Wind power in forests II: Forest wind.
[8] Kosovic B and Curry J A 2000 *J. Atmos. Sci.* **57** 1052–1068.
[9] Muñoz-Esparza D, Kosović B, Van Beeck J and Mirocha J 2015. *Phys. of Fluids* **27** 3, 035102.
[10] Zilitinkevich S, Esau I and Baklanov A 2002 *Q. J. R. Meteorol Soc.* **133** 265-271.
[11] Grisogono B 2011 *Q. J. R. Meteorol Soc.* **137** 700-708.
[12] Nieuwstadt, F T M 1984 *J. Atmos. Sci.* **41** 2202–2216.
[13] Weller HG, Tabor G, Jasak H and Fureby C 1998 *Computers in Physics* **12(6)**
[14] Deardorff J W 1980 *Boundary-Layer Meteorology*, **18(4)** 495-527 Springer
[15] Moeng C-H 1984 *Journal of the Atmospheric Sciences* **41(13)** 2052-2062.
[16] Schumann, U 1975 *Journal of computational physics* **18(4)** 376-404
[17] Basu S, Holtslag A A, Van De Wiel B J, Moene A F and Steeneveld G J 2008 *Acta Geophysica* **56** 88-99.
[18] Churchfield M J, Lee S and Fleming P 2012 available at https://www.nrel.gov/wind/nwtc/sowfa.html, created by National Renewable Energy Lab.(NREL) United States
[19] Nebenführ B and Davidson L 2015 *Boundary-Layer meteorology* **156** 253-276.
[20] Olivares-Espinosa H and Arnqvist J 2023 *Journal of Physics: Conference Series* **2505** 1.
[21] Olivares-Espinosa H, Arnqvist J and Ivanell S 2019 *J of Phys.: Conf. Series* **1256** 1, 012002